Heliyon 10 (2024) e38649

Contents lists available at ScienceDirect

Heliyon

journal homepage: www.cell.com/heliyon

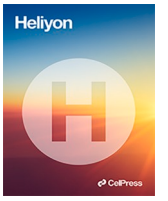

Research article

# Exploring synergistic effects of *Achyranthes bidentata* Blume and *Paeonia lactiflora* Pall. on hypertension with liver yang hyperactivity using the multidisciplinary integrative strategy

Yanyan Zhang [a,1], Peimei Yan [a,1], Yuhui He [a], Shan Ren [b], Dingxiao Wu [b], Yingwanqi Wang [a], Siyao Song [b], Peng Lu [b], Xue Li [c], Guangwei Li [b], Weiwei Jia [a], Ying Lyu [a], Haiying Dong [d], Dan Xiao [e], Lin Ding [f], Song Lin [a,g,**], Yan Lin [a,g,*]

[a] *Center of Scientific Research, School of Basic Medicine, Qiqihar Medical University, Qiqihar, 161006, China*
[b] *Department of Pathophysiology, School of Basic Medicine, Qiqihar Medical University, Qiqihar, 161006, China*
[c] *Department of Physiology, School of Basic Medicine, Qiqihar Medical University, Qiqihar, 161006, China*
[d] *Department of Clinical Pathology Diagnosis, Qiqihar Medical University, Qiqihar, 161006, China*
[e] *School of Medicine and Health, Harbin Institute of Technology, Harbin, 150000, China*
[f] *Department of Scientific Research, Science and Technology Achievement Transformation Center, Qiqihar Medical University, Qiqihar, 161006, China*
[g] *Key Laboratory of Homology of Medicine and Food Resources and Metabolic Disease Prevention and Treatment of Heilongjiang Province, Qiqihar, Heilongjiang Province, 161006, China*

ARTICLE INFO

*Keywords:*
*Achyranthes bidentata* Blume
*Paeonia lactiflora* Pall.
Principal component analysis
Metabolomics
16s rRNA
Weighted correlation network analysis
Hypertension

ABSTRACT

Traditional Chinese Medicine (TCM) formulations serve as a multi-component pharmacological combination therapy with various potential targets and have collected extensive knowledge regarding the in vivo efficacy of treating cardiovascular disorders in clinical practice for thousands of years. However, the obscurity of the chemicals and the molecular mechanisms are impediments to their continued growth and globalization. Therefore, new modern medications based on the combination of beneficial TCM components with precise clinical efficacy are required. The goal of this study was to find the best combination of *Achyranthes bidentata* Blume (AB) and *Paeonia lactiflora* Pall. (PL) for hypertension with liver yang hyperactivity (HLYH). The integrated research consisting of principal component analysis (PCA), metabolomics, microbiology, and weighted correlation network analysis (WGCNA) were used to find the optimal combination of AB-PL combinations and reveal the mechanism of action. The result showed AB-PL (2:3) had a substantial protective impact on HLYH, as shown by lower blood pressure, improved liver yang hyperactivity, reduced cardiac remodeling and malondialdehyde (MDA), and increased NO content. Furthermore, the essential elements for AB-PL reducing hypertension may be related to 135 metabolites and 23 microorganisms. In conclusion, our findings support the efficacy of herbal remedies in the treatment of hypertension and provide some pharmacological evidence for the ongoing development of novel modern Chinese drugs for cardiovascular disorders.

* Corresponding author. Center of Scientific Research, School of Basic Medicine, Qiqihar Medical University, Qiqihar, 161006, China.
** Corresponding author. Center of Scientific Research, School of Basic Medicine, Qiqihar Medical University, Qiqihar, 161006, China.
*E-mail addresses:* linsong0228@163.com (S. Lin), yanlinqqhr@aliyun.com (Y. Lin).
[1] These authors contributed equally to this study.

https://doi.org/10.1016/j.heliyon.2024.e38649
Received 27 January 2024; Received in revised form 5 September 2024; Accepted 26 September 2024
Available online 5 October 2024

## 1. Introduction

Hypertension, a significant contributor to cardiovascular ailments, stands as a prominent risk factor for morbidity and mortality on a global scale. This intricate condition manifests as a persistent elevation of arterial blood pressure, potentially leading to detrimental consequences for the kidneys, brain, and vascular system, thereby heightening the susceptibility to hypertension [1]. However, the underlying mechanisms of hypertension remain incompletely elucidated. Thus, comprehending the etiology and discovering novel approaches for managing hypertension will profoundly influence the overall well-being and vitality of individuals. Traditional Chinese Medicine (TCM) has advantages for hypertension diagnosis and treatment, such as personalized and precise treatment with few side effects, and herb pairings are widely used in TCM prescriptions [2]. TCM prescription ZhenGanXiFeng decoction (ZGFD), composed of twelve species of Chinese medicines, also known as the "Sedate the Liver and Extinguish Wind Decoction", has been used for millennia to treat hypertension of different syndrome types [3,4]. Hypertension with liver yang hyperactivity (HLYH) is a prevalent ailment characterized by elevated blood pressure and manifestations such as headaches, dizziness, restlessness, and palpitations [5]. TCM therapy encompasses the principles of "calming the liver," "dispelling wind," "clearing heat," and "promoting blood circulation" [6].

*Achyranthes bidentata* Blume (AB) and *Paeonia lactiflora* Pall. (PL), well-known for their liver-soothing and wind-extinguishing characteristics, are the essential medication pairs of ZGFD. Studies have shown that AB could dredge muscles, replenish the liver and kidneys, and has anti-hyperlipidemia, antioxidant, and anti-inflammatory qualities in addition to having a clear antihypertensive effect [7]. The main components of AB, total saponins, are directly linked to NO-mediated vasodilation. In addition to avoiding sweating, softening the liver to relieve pain and inhibiting liver yang, PL has blood-tonic properties and is widespread used in clinical practice [8,9]. Numerous pharmacological activities, including anti-inflammatory and analgesic effects, enhancing NO production, and relieving cardiac hypertrophy, are exhibited by the well-known pharmaceutical substances PL [10,11]. Consequently, conducting antihypertensive research on AB-PL drug pair may be a promising effective method for achieving hypertension treatment. However, the synergistic mechanisms of AB-PL have not yet been described.

In our present investigation, employing the approach of multidisciplinary integration, our aim was to explore the optimal compatibility and mechanism of the synergistic impact of AB-PL on N-Nitro-L-Arginine Methyl Ester (L-NAME) induced HLYH. Integration analysis of microbiology, metabolites and WGCNA can provide a theoretical basis for the treatment of HLYH.

## 2. Materials and methods

### 2.1. Chemicals and reagents

Both *Achyranthes bidentata* Blume dispensing granule (batch number: 1013141, 2.5 g of *Achyranthes bidentata* Blume dispensing granule is equivalent to 10 g of crude drug of AB decoction pieces for clinical treatment.) and *Paeonia lactiflora* Pall. dispensing granule (batch number: 0129411, 1 g of *Paeonia lactiflora* Pall. dispensing granule is equivalent to 10 g of crude drug of PL decoction pieces for clinical treatment.) were purchased from Guangzhou Yifang Pharmaceutical Co., Ltd. An extract of *Aconitum carmichaelii* Debeaux

**Table 1**
Information of AB-PL major components. Mass error of components were not greater than 10 ppm.

| NO. | Compound | Formula | $t_R$/min | *m/z* | Mass error |
|---|---|---|---|---|---|
| 1 | Chrysophanic acid | $C_{15}H_{10}O_4$ | 1.6 | 255.0656 | 1.5 |
| 2 | Palmitic acid | $C_{16}H_{32}O_2$ | 2.0 | 227.2005 | 1.2 |
| 3 | benzoic acid | $C_7H_6O_2$ | 2.2 | 257.2485 | 1.7 |
| 4 | Mudanpioside C | $C_{30}H_{32}O_{13}$ | 2.4 | 601.1941 | 3.1 |
| 5 | 6′-O-Galloyl paeoniflorin | $C_{30}H_{32}O_{15}$ | 4.1 | 633.1841 | 3.3 |
| 6 | Paeonolide | $C_{20}H_{28}O_{12}$ | 4.3 | 461.1678 | 3.9 |
| 7 | naringenin | $C_{15}H_{12}O_5$ | 4.9 | 273.0772 | 3.0 |
| 8 | Cyasterone | $C_{29}H_{44}O_8$ | 5.2 | 521.3126 | 2.2 |
| 9 | Gallic acid | $C_7H_6O_5$ | 5.3 | 171.0297 | 1.6 |
| 10 | Lactiflorin | $C_{23}H_{26}O_{10}$ | 5.6 | 463.1611 | 1.2 |
| 11 | Benzoylpaeoniflorin | $C_{30}H_{32}O_{12}$ | 5.8 | 585.1988 | 2.5 |
| 12 | albiflorin | $C_{23}H_{28}O_{11}$ | 6.0 | 481.1724 | 2.6 |
| 13 | β-ecdysterone | $C_{27}H_{44}O_7$ | 6.0 | 481.3160 | 3.3 |
| 14 | Paeoniflorin | $C_{23}H_{28}O_{11}$ | 6.1 | 481.1729 | 3.7 |
| 15 | 25-Inokosterone | $C_{27}H_{44}O_7$ | 6.1 | 481.3179 | 2.6 |
| 16 | Oxypaeoniflorin | $C_{23}H_{28}O_{12}$ | 6.1 | 497.1670 | 2.1 |
| 17 | Paeonol | $C_9H_{10}O_3$ | 6.5 | 167.0712 | 1.9 |
| 18 | alpha-Spinasterol | $C_{29}H_{48}O$ | 6.7 | 413.3791 | 1.6 |
| 19 | 5-hydroxymethylfurfural | $C_6H_6O_3$ | 6.8 | 127.0398 | 1.4 |
| 20 | Benzoylpaeoniflorin | $C_{30}H_{32}O_{12}$ | 7.6 | 585.1989 | 2.8 |
| 21 | Tocopherols | $C_{29}H_{50}O_2$ | 8.5 | 431.3908 | 4.1 |
| 22 | Chikusetsusaponin IVa | $C_{42}H_{66}O_{14}$ | 9.0 | 795.4568 | 4.5 |
| 23 | Ginsenoside Ro | $C_{48}H_{76}O_{19}$ | 9.0 | 957.5095 | 3.7 |
| 24 | Nobiletin | $C_{21}H_{22}O_8$ | 9.5 | 403.1407 | 3.2 |
| 25 | 1,2,3,4,6-O-Pentagalloylglucose | $C_{41}H_{32}O_{26}$ | 10.1 | 941.1295 | 3.6 |
| 26 | Beta-Sitosterol | $C_{30}H_{52}O$ | 20.7 | 415.3952 | 2.7 |

(Aconitum) was obtained from the Qiqihar City Hospital of Traditional Chinese Medicine. The plants name have been checked with http://MPNS.kew.org. L-NAME with purity ≥98 % (batch number: N5751), purchased from Sigma Aldrich (Shanghai) Trading Co., Ltd., Masson Tricolor Staining Kit (product number: G1340), purchased from Beijing Solaybao Technology Co., Ltd., ANP and BNP kits (product numbers: JL20612, JL12884), purchased from Shanghai Jianglai Biotechnology Co., Ltd., and malondialdehyde and NO kits (product numbers: S0131S, S0021S), purchased from Beyotime Institute of Biotechnology (Shanghai) Co. Ltd.

### 2.2. The analysis of major components of AB-PL

The major components of AB-PL were analyzed through a HPLC-ESI-Q/TOF-MS system. Chromatography analysis was consisted of a LC-20 A Prominence™ UFLC XR system (Shimadzu, Kyoto, Japan) equipped with the ACQUITY UPLC HSS T3 C18 column (2.1 × 100 mm, 1.7 μm, Waters, Milford, MA, USA). TripleTOF™ 4600 (Sciex, Foster City, CA, USA) was used in both *positive-ion-mode* electrospray ionization ($ESI^+$) and *negative-ion-mode* electrospray ionization ($ESI^-$) modes. In the $ESI^+$ mode, the Ionspray voltage floating, the turbo spray temperature, Declustering potential, Collision gas, Nebulizer gas, Heater gas and Curtain gas are 5500 V, 550 °C, 100 V, 30eV, 50psi, 50psi, 30psi respectively. 5500 V, 550 °C, 100 V, 30eV, 50psi, 50psi, 30psi. In $ESI^-$ mode these parameters are −4500 V, 550 °C, −80 V, −10eV, 50psi, 50psi, 30psi.

In the liquid phase, the column was kept at 35 °C with a flow rate of 0.35 ml $min^{-1}$. Mobile phase A was 0.1 % formic acid in water, and mobile phase B was 0.1 % formic acid in acetonitrile. The elution gradient was: 10–35 % B (0–2 min), 35–70 % B (2–5 min, held for 5 min), then returned to 95 % B and maintained until 15 min. The TOF MS scan comprised a mass range of *m/z* 50–1200.

The mass spectrum was acquired under typical information-dependent acquisition (IDA) conditions for the MS/MS experiment. The optimized MS parameters were as Table 1. Nitrogen served as both the nebulizer and auxiliary gas, and the operations were conducted using Analyst software (version 1.7, Sciex).

### 2.3. Animal models and drug intervention

96 Kunming mice (18–22 g), 6 weeks of age, were supplied by the Animal Research Institute of Qiqihar Medical University (Experimental Animal Licencing Number: SYXK 2021-013, Ethical approval number: QMU-AECC-2022-115). The mice were kept under standard laboratory conditions, which comprised a 12/12 light-dark cycle, temperatures between 22 ± 2 °C, relative humidity levels between 45 ± 5 %, as well as free access to food and water. All experimental animals were acclimatized for 7 days before the experiment. Then 96 mice were randomly divided into 8 groups of 12 mice each. Aconitum and L-NAME were administered by gavage at a dose of 2.8 g $kg^{-1}$ and 60 mg $kg^{-1}$, respectively [12,13]. AB-PL formulated granules were dissolved in distilled water, and according to the recommended dosage of ZGXF, the settings for each administration group are as follows (calculated based on the amount of raw medicine) were 5 : 0 (AB:PL = 6.825 g $kg^{-1}$: 0 g·$kg^{-1}$), 4 : 1 (AB:PL = 5.46 g $kg^{-1}$: 1.365 g $kg^{-1}$), 3 : 2 (AB:PL = 4.095 g $kg^{-1}$: 2.73 g $kg^{-1}$), 2 : 3 (AB:PL = 2.73 g $kg^{-1}$: 4.095 g $kg^{-1}$), 1 : 4 (AB:PL = 1.365 g $kg^{-1}$: 5.46 g $kg^{-1}$) and 0 : 5 (AB:PL = 0 g·$kg^{-1}$: 6.825 g $kg^{-1}$). Control group were given the same dose of saline by gavage. AB-PL different ratio groups were administered by gavage at the same time as modeling for 6 weeks. Finally, the mice were executed 12 h after the last administration, and their blood and hearts were obtained.

### 2.4. Tests for experimental indices

Facial temperature and water intake of the mice were measured during the first and sixth week. Meanwhile, at the end of the sixth week, the mice's irritability level, rotation time, whether the color of the conjunctiva of both eyes deepened and turned red, and whether the fur color was shiny were measured [14,15]. The degree of agitation was categorized into three levels: Level I refers to screaming and jumping when catching and holding the neck; Level II refers to biting when catching and holding the neck; and Level III refers to screaming and jumping when the tail is lifted, and even frequently fighting or biting other mice in the same cage. The level of vertigo was assessed by testing the mice's rotation time. (Specifically place the mice on a platform spinning at 45 revolutions per minute and record the time it takes them to drop.) Mice were placed on a platform spinning at 45 revolutions per minute and the time it took for them to drop was recorded. If the mice remained stable for 2 min, the experiment was over [16]. Facial temperature was detected with the help of an infrared thermometer. The infrared thermometer was attached to the area between the mouse's mouth and ear to measure the mice's facial temperature [14]. Three measurements were taken for each mouse and the average temperature was calculated from the measurements. In addition, the water intake of the mice was tracked three days a week [17]. Finally, the facial temperature and water intake obtained in the first week were subtracted from the sixth week to obtain the changes in the corresponding indices of the mice.

### 2.5. Blood pressure measurement

Systolic blood pressure and diastolic blood pressure of mouse caudal artery blood pressure were detected by noninvasive computerized tail-cuff system (Kent Scientific Co., Ltd., America) [18]. The mice were confined in a restrainer that was set up on a heated plate in a groove. The VPR sensor was positioned 1 cm below the O-Cuff sensor. The tail of mice was kept at a temperature of 30 ± 2 °C for the measurements. The device took measures of blood pressure and heart rate 30 times automatically.

### 2.6. Tissue collection and analysis

Mice were euthanized by intraperitoneal injection of a lethal dose of pentobarbital, then perfused intracardiacally with cold 4 % paraformaldehyde (in PBS), and heart tissue were excised and fixed in 4 % paraformaldehyde for histopathology studies. Heart weight/body weight ratio (HW/BW, mg/g), and heart weight/tibia length (HW/TL, mg/mm) were calculated for each cohort by weighing the hearts and body.

### 2.7. Hematoxylin-eosin (HE) and Masson staining

The heart tissue was fixed in formalin and embedded in paraffin. Sections with a thickness of 5 μm were prepared and subjected to HE and Masson staining. The tissue changes were evaluated using an optical microscope and imaging (Leica, DM2000, Germany) to assess histological alterations. HE staining was primarily used to observe changes in myocardial tissue structure and the size of myocardial cells. Masson staining, on the other hand, was mainly employed to evaluate myocardial fibrosis in the tissue.

### 2.8. Enzyme-linked immunosorbent assay (ELISA) analysis

After treatment, myocardial tissue homogenate was collected. Tissue levels of atrial natriuretic peptide (ANP), and B-type natriuretic peptide (BNP) were measured by the corresponding ELISA Kits, according to manufacturer's instruction.

### 2.9. Assays for nitric oxide (NO) and malondialdehyde (MDA) content

Myocardial tissue was collected and washed with ice-cold PBS. The tissue was then incubated with lysis buffer on ice for 30 min. Afterward, the tissue lysates were centrifuged at 8000×*g* for 10 min at 4 °C. The supernatant was collected and the content of NO and MDA were assayed by commercially available assay kits according to the manufacturer's instructions.

### 2.10. Metabolomics

Metabolomics was conducted by Biotree Profile (Shanghai, China). Briefly, 25 mg sample was placed in an EP tube, followed by the addition of 500 μL of an extract solution (methanol: acetonitrile: water = 2: 2: 1, with an isotopically-labelled internal standard mixture). The mixture was homogenized at 35 Hz for 4 min and then sonicated for 5 min in an ice-water bath. This homogenization and sonication process was repeated three times. Subsequently, the samples were incubated for 1 h at −40 °C and centrifuged at 12000 rpm for 15 min at 4 °C. The resulting supernatant was transferred to a new glass vial for analysis. A quality control (QC) sample was prepared by combining equal aliquots of the supernatants from all the samples.

LC-MS/MS analyses were conducted utilizing a UHPLC system (Vanquish, Thermo Fisher Scientific) with a Waters BEH Amide column (2.1 mm × 50 mm, 1.7 μm) coupled to an Orbitrap Exploris 120 mass spectrometer (Orbitrap MS, Thermo). The mobile phase, consisting of 25 mmol/L ammonium acetate and 25 ammonia hydroxide in water (pH = 9.75) (A) and acetonitrile (B), facilitated separation. The auto-sampler was maintained at 4 °C, with an injection volume of 2 μL. The Orbitrap Exploris 120 mass spectrometer, employed for its MS/MS capabilities in information-dependent acquisition (IDA) mode, was controlled by Xcalibur software. The ESI source conditions included a sheath gas flow rate of 50 Arb, Aux gas flow rate of 15 Arb, capillary temperature of 350 °C, full MS resolution of 60000, MS/MS resolution of 30000, collision energy set at 20/30/40 in NCE mode, and spray voltage at 3 kV (positive) or −3 kV (negative), respectively. The elute gradient was set as follows: 10 % B from 0 to 1 min, 10–95 % B from 1.01 to 10 min, 95 % B from 10.01 to 13 min, and 95–10 % B from 13.01 to 15 min.

The initial data in ProteoWizard were transformed into the mzXML format, and subsequent processing involved an in-house program created in R, utilizing XCMS for peak detection, extraction, alignment, and integration. Metabolite annotation employed an in-house MS2 database (BiotreeDB), with an annotation cutoff set at 0.3 for accuracy.

### 2.11. Microbiomics

16S rRNA sequencing of mice stool samples were conducted by Biotree Profile (Shanghai, China). In short, stool samples were processed for total genomic DNA extraction using the CTAB/SDS method. The DNA concentration and purity were assessed on 1 % agarose gels, and the extracted DNA was diluted to 1 ng $\mu L^{-1}$ with sterile water. PCR amplification targeted the V3-V4 region of the 16S rRNA gene using Phusion® High-Fidelity PCR Master Mix. PCR products were visualized on a 2 % agarose gel, purified with the Qiagen Gel Extraction Kit, and utilized for library construction with the TruSeq DNA PCR-Free Sample Preparation Kit (Illumina, USA). Library quality was evaluated on an Agilent Bioanalyzer 2100 system, and Illumina NovaSeq facilitated 16S rRNA V4 sequencing. Data processing was conducted using QIIME (Version 1.7.0) and R software (Version 2.15.3).

### 2.12. Weighted correlation network analysis (WGCNA)

Subsequently, WGCNA and CytoHubba were applied for investigating potential mechanisms of AB-PL on hypertension with hyperactive liver-yang syndrome [19]. The relationship between module traits and metabolites/microfloras was explored by using the WGCNA package, where the scale-free R2, cut height, and minimum module size was set to 0.95, 0.25, and 10, respectively, to identify

important modules. MetaboAnalyst (http://www.metabo-analyst.ca/) was used for pathway enrichment analysis (parameters set to default values). CytoHubba applications in Cytoscape (v.3.8.2) were used to search for significant metabolites and microfloras, with default parameters [20,21].

### 2.13. Statistical analysis

Data were shown as mean ± Standard Error of the Mean (SEM) from at least 4 independent experiments. An unpaired *t*-test was used for comparison between the two groups. $P < 0.05$ was considered statistically significant. Utilizing SIMCA-P (version14.0, Umetrics, Umea, Sweden), 14 main pharmacodynamic indicators, such as differences in systolic blood pressure, differences in diastolic blood pressure, and so on, which were affected by different combinations of drugs, were used as variables for PCA. The first principal component (FPC) was extracted to evaluate the efficacy differences between different compatibility ratios of AB and PL.

## 3. Result

### 3.1. AB-PL improves the symptoms of liver yang hyperactivity and blood pressure of mice

First, the major components of AB-PL were characterized by HPLC-ESI-Q/TOF-MS (Table 1 and Fig. 1). Then, we investigated the effects of AB-PL on symptoms of liver yang hyperactivity by assessing the physical signs of mice. We found that irritability levels, hyperemia of conjunctiva and dry hair of mice were more severe in HLYH group compared with control group, upon treatment with AB-PL (4:1, 3:2, 2:3 and 1:4), the physical signs were gradually improved in mice. As shown in Fig. 2A–C, compared with the control group, the rotation time was decreased and water intake and face temperature were increased significantly in the HLYH group ($P < 0.01$). Compared with the HLYH group, the AB-PL (2:3) treatment group exhibited a longer rotation time ($P < 0.05$), indicating that headache and facial flushing vertigo were alleviated, meanwhile, water intake were decreased in the AB-PL different ratio treatment groups ($P < 0.05$, 0.01).

As shown in Fig. 2D and E, comparison before and after the experiment, the HLYH group exhibited a higher difference of tail artery systolic and diastolic blood pressure than the control group ($P < 0.05$,0.01). The AB-PL (2:3) treatment group had lower systolic and diastolic blood pressure differences compared to the HLYH group ($P < 0.05$), indicating an effective inhibition of elevated blood pressure.

### 3.2. AB-PL ameliorates myocardial remodeling in L-NAME induced HLYH mice

Prolonged elevation of blood pressure can lead to cardiomyocyte hypertrophy and myocardial fibrosis, which can have a detrimental effect on the contraction and relaxation functions of the heart [22]. Comparing to the control group, there was an increase the ratio of HW/BW, HW/TL and the level of ANP, BNP were increased in HLYH group. In addition, AB-PL (2:3) treatment group significantly decreased the ratio of HW/BW, HW/TL and the level of ANP, BNP as compared with HLYH group ($P < 0.05$,0.01) (Fig. 3A–D).

Fig. 3E–H displays the results of HE and Masson staining of the heart. In the control group, myocardial cells exhibited regular and well-defined arrangement. No significant degenerative hyperplasia was detected in the collagen fibers of intercellular substances in the

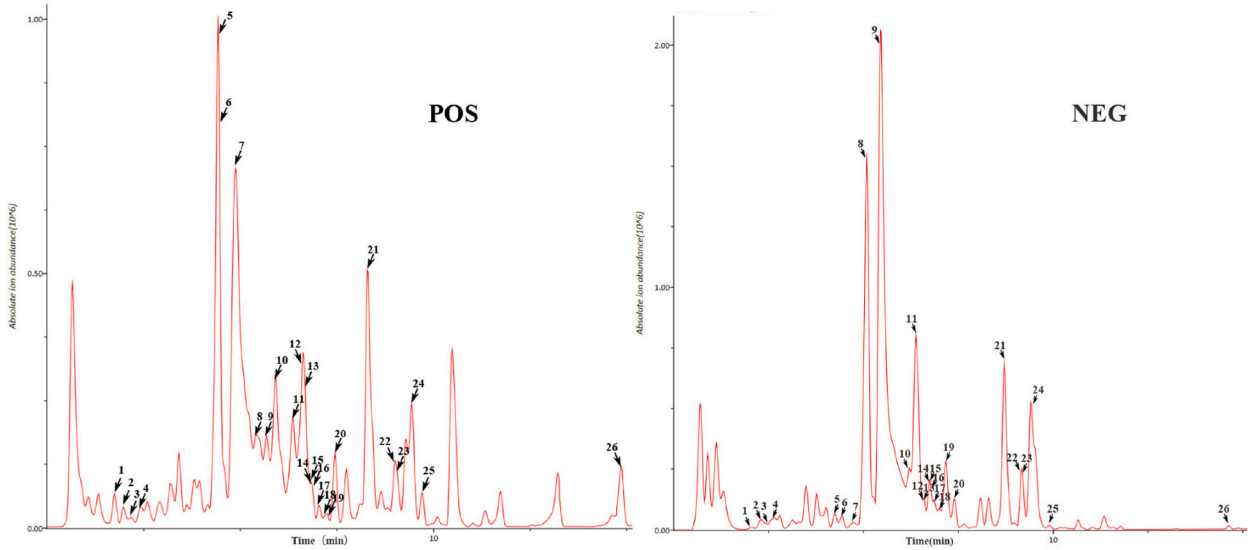


**Fig. 1.** The total ion chromatogram of AB-PL in positive (A) and negative (B) mode.

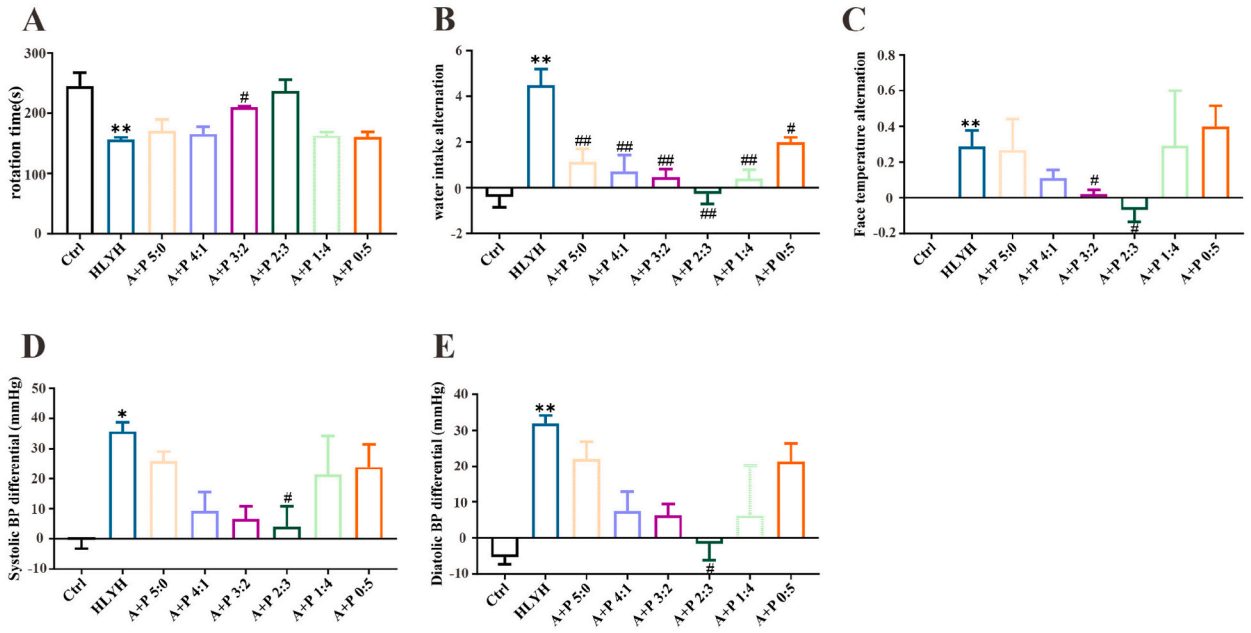


**Fig. 2.** The results of time of rotating rod (A), drinking water (B) and face temperature (C), difference of systolic blood pressure (D), difference of diastolic blood pressure differential (E) in control group, HLYH group, and AB-PL treatment groups (5:0, 4:1, 3:2, 2:3, 1:4, 0:5). ($n \geq 4$, $^{*}P < 0.05$, $^{**}P < 0.01$ vs the control group, $^{\#}P < 0.05$, $^{\#\#}P < 0.01$ vs HLYH group).

control group. However, the HLYH group exhibited irregular myocardial cell arrangement, pronounced infiltration of inflammatory cells, numerous collagen fibers were observed occupying the interstitial spaces of the myocardium. Additionally, some myocardial cells exhibited significant hypertrophy. AB-PL treatment markedly decreased inflammatory infiltration and fibrosis compared to the HLYH group. These results indicate that the combination of these two drugs effectively ameliorates myocardial fibrosis in L-NAME-induced HLYH mice. Notably, AB-PL (2:3) showcased a more orderly arrangement of myocardial fibers and displayed a significant decrease in collagen content.

### 3.3. AB-PL reverses the contents of MDA and NO

As depicted in Fig. 4A and B, compared with the control group, the content of MDA was increased and the level of NO was decreased statistically in HLYH group ($P < 0.05$).

Compared with HLYH group, the contents of MDA and NO were reversed in AB-PL (2:3 and 3:2) treatment group ($P < 0.05$, 0.01).

### 3.4. Principal component analysis

The 14 indicators mentioned above were subjected to data standardization for PCA. The PCA result showed a separation trend among the control group, HLYH group, and AB-PL groups with ratios of 0:5, 2:3, 3:2, and 5:0 (Fig. 5A). The results clearly indicated notable variations in protective effects among the six aforementioned groups, highlighting significant differences among them. Additionally, to systematically simplify the complexity of the study and identify indicators that could effectively reflect the effects of different combinations of AB-PL, the characteristic values, variance contribution rates, and cumulative contribution rates of principal components for anti-hypertension in each group were computed. As the total variance explained in, the characteristic value λ of the first principal component (FPC) was 5.44. In the dimensionality reduction process of PCA, it was considered that principal components, which were with characteristic values ≥ 1, could represent the characteristics of the data. Therefore, FPC was recommended as a key indicator of efficacy for different combinations of AB-PL. Based on the principal component coefficients, a linear combination of FPC was established (Table S2). Consequently, the corresponding FPC for each sample was calculated (Fig. 5B). The results showed that the HLYH group had the highest mean FPC value, while the mean FPC value of the control group was the lowest, and the mean FPC values of each treatment group were between the control and HLYH groups. The above results indicated that the FPC value was closely related to the degree of HLYH, which meant that a lower FPC value might indicate that the organism was closer to a normal state. In other words, FPC value could be used as a comprehensive pharmacological evaluation indicator to determine treatment effectiveness, i.e., a lower FPC value indicated a better protective effect of drugs. So according to FPC values, the ranking of the protective ability of different combinations of AB-PL for HLYH was as follows: AB-PL 2:3 group > AB-PL 3:2 group > AB-PL 4:1 group > AB-PL1:4 group > AB-PL 5:0 group > AB-PL 0:5 group.

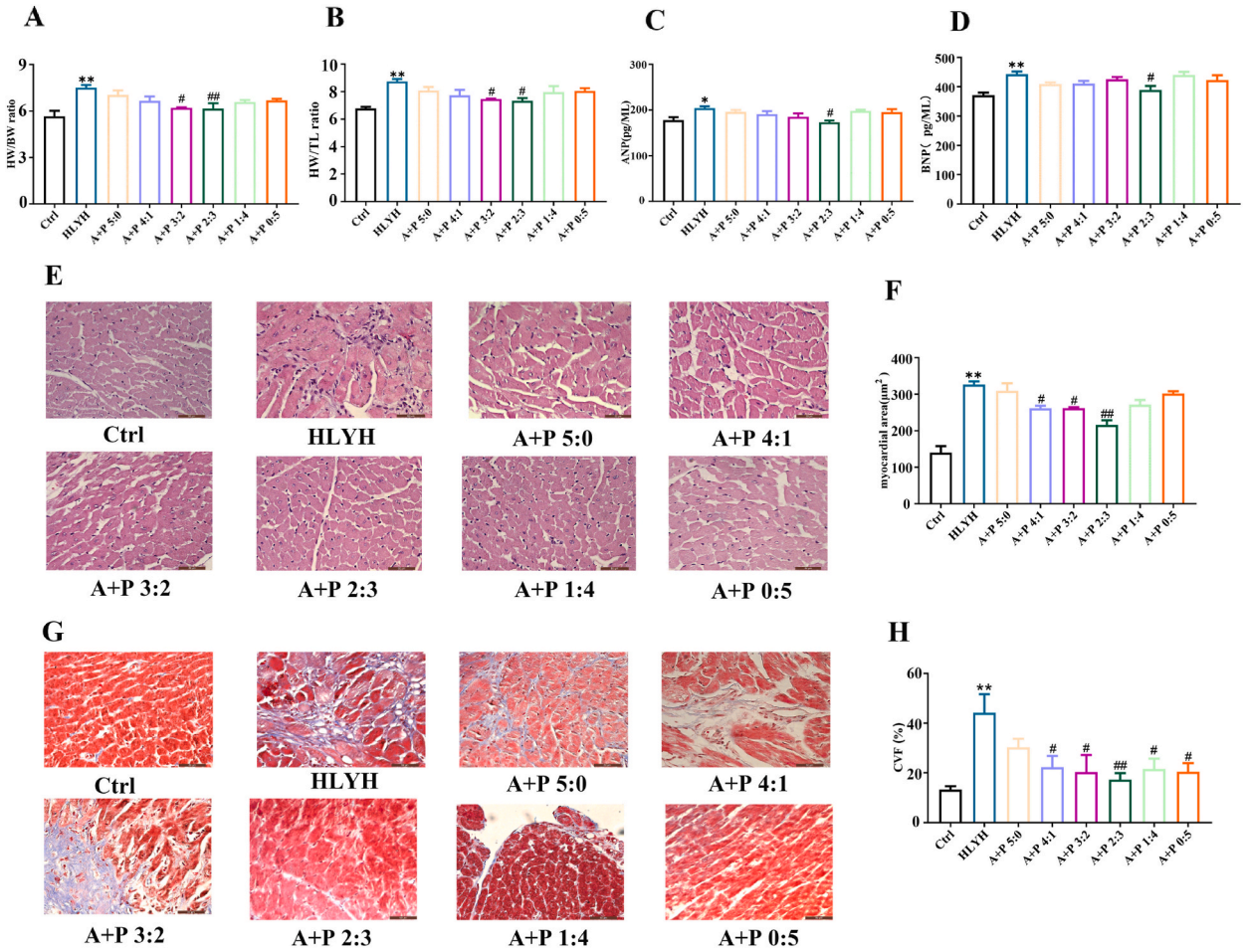


**Fig. 3.** Ratio of HW/BW (A), ration of HW/TL (B), level of ANP (C) and BNP (D) of mice and effect of AB-PL with different ratio on myocardial area (E and F) and myocardial fibrosis (G and H) of HLYH mice. (HE & Masson, 40 × , E: myocardial area, F: the results of myocardial area, G: myocardial fibrosis, H: the results of myocardial fibrosis. n ≥ 6, $^{*}P < 0.05$, $^{**}P < 0.01$ vs the control group, $^{\#}P < 0.05$, $^{\#\#}P < 0.01$ vs HLYH group).

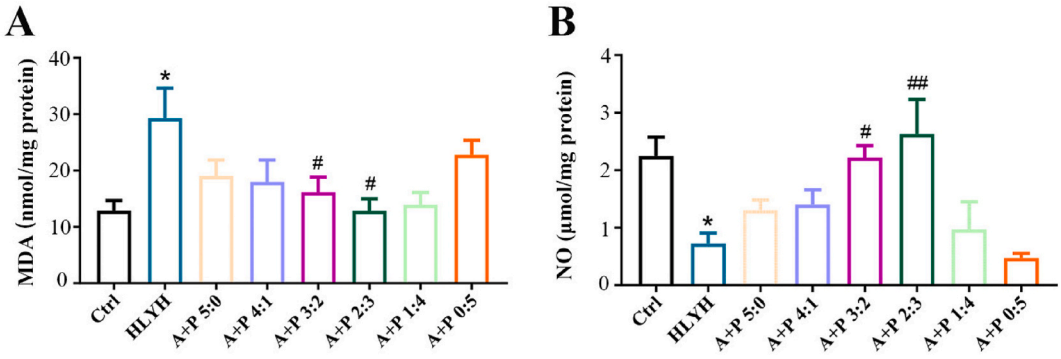


**Fig. 4.** The effects of different ratio of AB-PL on MDA (A), and NO (B) in hypertensive mouse myocardium. (n ≥ 6, $^{*}P < 0.05$ vs the control group, $^{\#}P < 0.05$, $^{\#\#}P < 0.01$ vs HLYH group).

### *3.5. The establishment and analysis of the weighted co-expression network*

As shown in Fig. 6A and Fig. S1, QC samples represented fine responses and significant aggregation demonstrating the reliability of the metabolomic method. Furthermore, there were remarkable disparities in the metabolic profiles of the samples across different

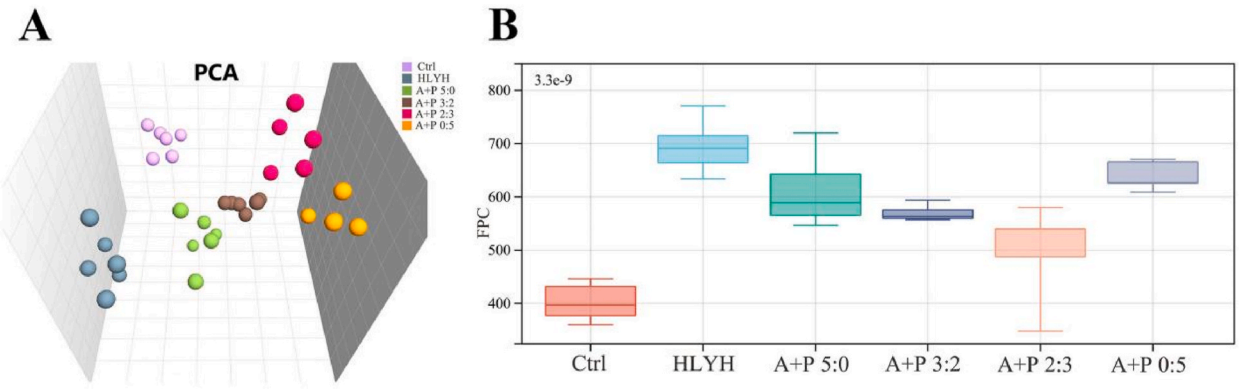


**Fig. 5.** PCA (A) and FPC (B) of different combinations of AB-PL.

treatment groups, suggesting variations in the protective effects of different drug combinations. Finally, 722 metabolites were achieved in the metabolomic analysis based on accurate mass and MS/MS information (Table S2). In addition, 16s rRNA analysis showed different ratio of AB-PL resulted in differential changes in α and β diversity among each group, which also inferred distinctions in the effects of different combinations of drugs on microbial community structure (Fig. 6B and C). Next, a weighted correlation network analysis (WGCNA), based on a total of 722 metabolites and the top 30 microfloras with the greatest relative abundance at various taxonomic levels (including phylum, class, order, family, genus, and species), was conducted to explore the possible connection between these metabolites/microbial communities and their protective impact on AB-PL. The effectiveness of FPS was used as an indicator for measuring the protective effect. The results demonstrated a soft-thresholding power of 10 was applied, resulting in the identification of 11 modules (metabolites in the grey module were not clustered) (Fig. S1 and Fig. 7). The module-trait correlation

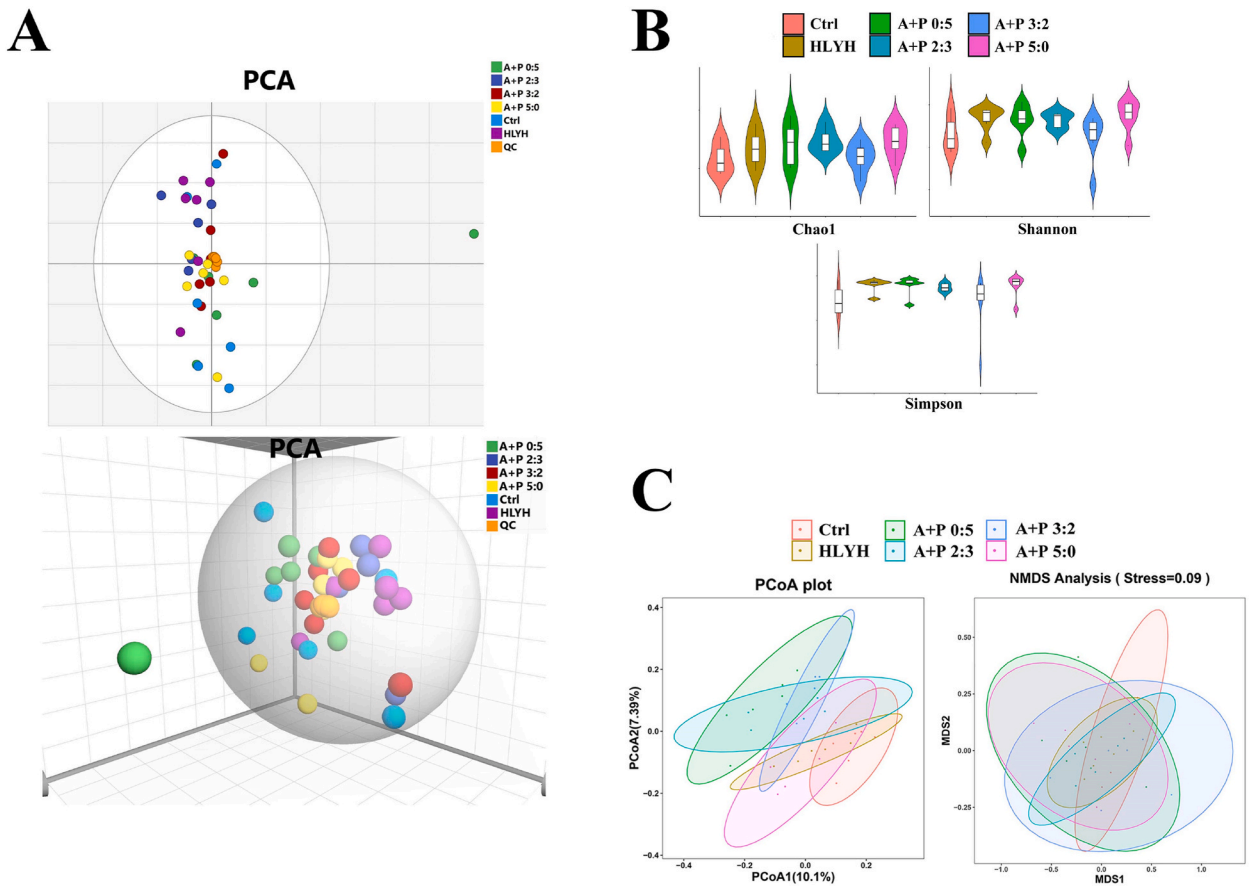


**Fig. 6.** PCA score plot of metabolomic analysis (A); α diversity analysis (B) and β diversity analysis(C) of 16s rRNA analysis.

results indicated that the red module, consisting of 59 metabolites and 16 microbial communities, as well as the green module, consisting of 76 metabolites and 7 bacterial groups, exhibited higher correlations with the protective effect of AB-PL (Figs. 7, 8A and 8B). Furthermore, the highly significant correlation between metabolites/microbiotas and module membership (MM) in the red or green modules indicated that metabolites/microbiotas highly associated with the protective effect of AB-PL were also significant members within the red or green modules. These findings attributed the red and green modules as important factors contributing to the treatment mechanism of AB-PL, warranting further exploration of these modules to identify key metabolites or microbiotas implicated in the protective effect of AB-PL.

### 3.6. The analysis of the significant module

To begin with, Metaboanalyst was utilized to conduct pathway analysis, which unveiled the metabolic pathways implicated in the red and green modules. As shown in Fig. 9i and 9ii, the red module was associated with pathways such as arginine biosynthesis, histidine metabolism, primary bile acid biosynthesis, taurine and hypotaurine metabolism. The green module was associated with glycerophospholipid metabolism, phenylalanine metabolism, arginine and proline metabolism, linoleic acid metabolism and so on. The prevention and treatment of AB-PL for hypertension with liver yang hyperactivity might depend on above pathways. Then, to identify key metabolites within the red and green modules, CytoHubba was utilized (Fig. 10A and B). Significant metabolites were selected by considering the overlap among the top 10 metabolites as determined by MCC score, Degree value, and MM value. In the red module, significant metabolites included beta-Alanyl-L-lysine, Valyl-Valine, Glycylleucine and gut Myxococcota. In the green module, significant metabolites included Tetradecanoylcarnitine, Stearoylcarnitine, and L-Palmitoylcarnitine. These metabolites and gut microbiota were regarded as important markers in the context of treatment of AB-PL for hypertension with liver yang hyperactivity.

## 4. Discussion

In this study, we have demonstrated that (1) AB-PL drug pair significantly decreased the syndrome of liver yang hyperactivity and alleviated the high blood pressure and cardiac remodeling induced by L-NAME HLYH. (2) AB-PL drug pair with a ratio of 2:3 demonstrated the most protective effect in treating HLYH using PCA. (3) The significant metabolites and gut microbiotas including beta-Alanyl-L-lysine, Valyl-Valine, Glycylleucine, Tetradecanoylcarnitine, Stearoylcarnitine, L-Palmitoylcarnitine and clostridium played crucial roles in the prevention of HLYH. This study determined the best synergistic effect and mechanism of the AB-PL drug pair

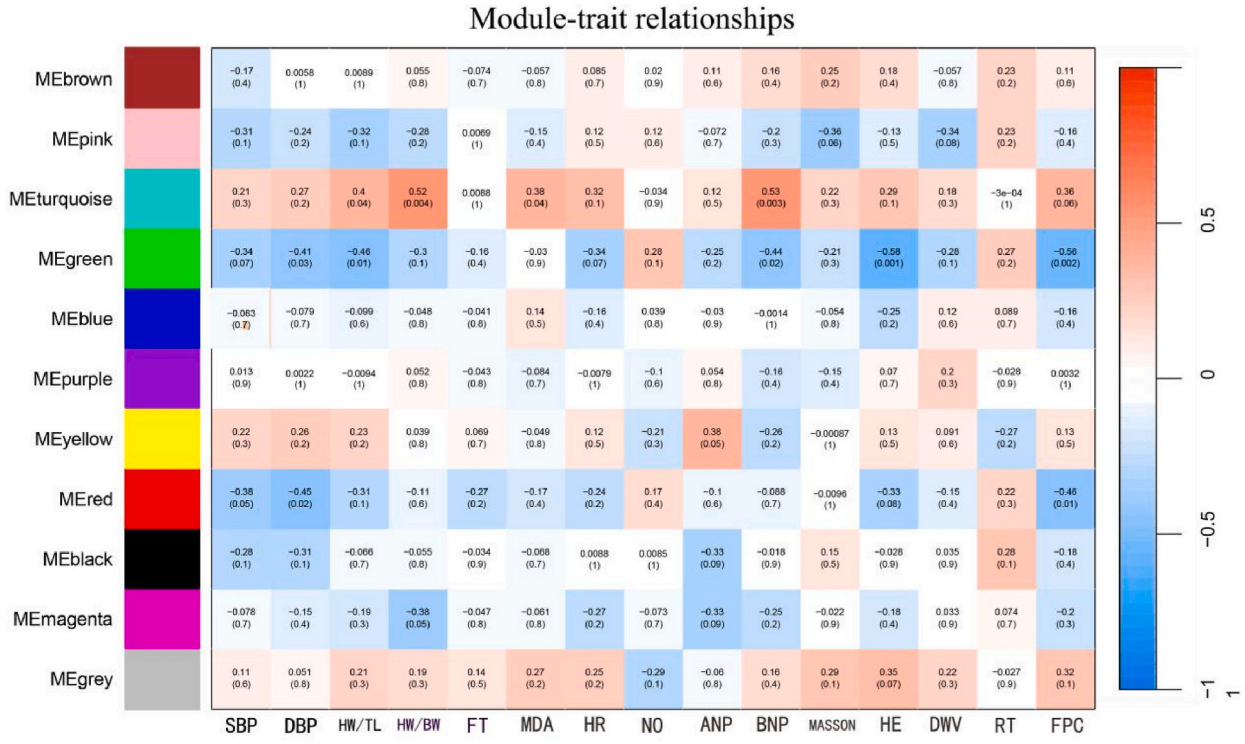


**Fig. 7.** Correlation heatmap between modules and traits. SBP: systolic blood pressure differential, DBP: diastolic blood pressure differential, HW/TL: heart weight/tibia length, HW/BW: heart weight/body weight ratio, FT: face temperature, MDA: malondialdehyde, HR: heart rate, NO: nitric oxide, ANP: atrial natriuretic peptide, BNP: brain natriuretic peptide, Masson: masson staining, HE: H&E staining, DWV: drinking water volume, RT: rotation time, FPC: first principal component.

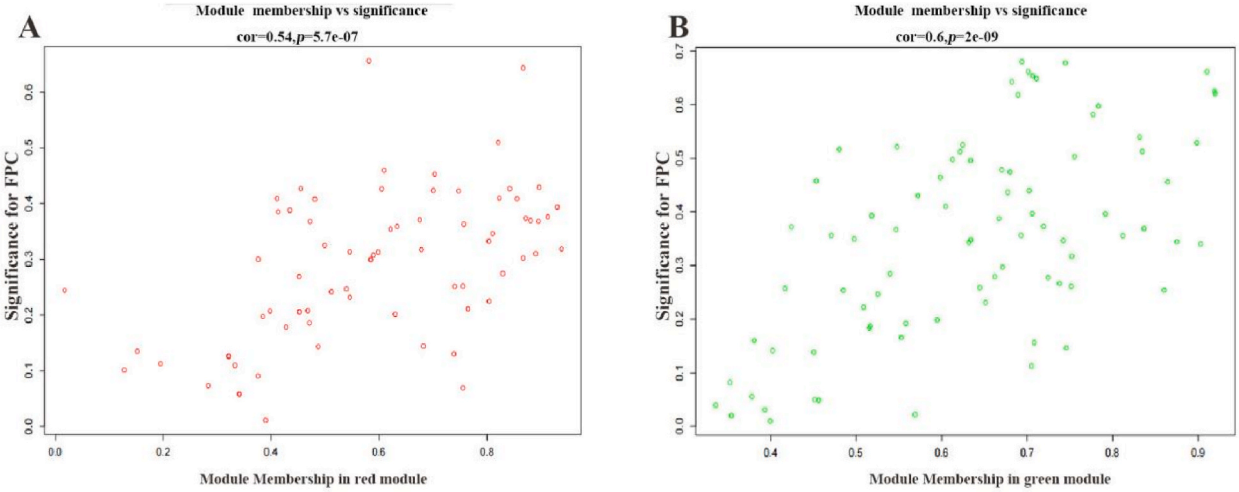


**Fig. 8.** Scatterplot of metabolite significance (y-axis) vs. module membership (x-axis) in red (A) and green (B) module.

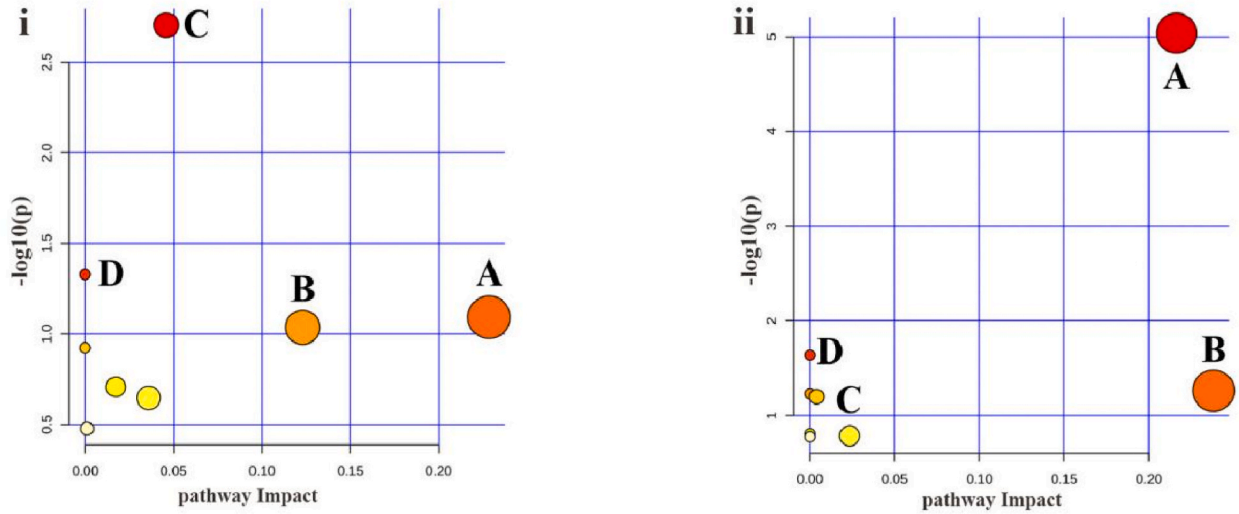


**Fig. 9.** Pathway analysis of metabolites. The pathways involved in the red module (i): A: Arginine biosynthesis; B: Histidine metabolism; C: Primary bile acid biosynthesis; D: Taurine and hypotaurine metabolism. The pathways involved in the green module (ii) A:Glycerophospholipid metabolism; B: Phenylalanine metabolism; C: Arginine and proline metabolism; D: Linoleic acid metabolism.

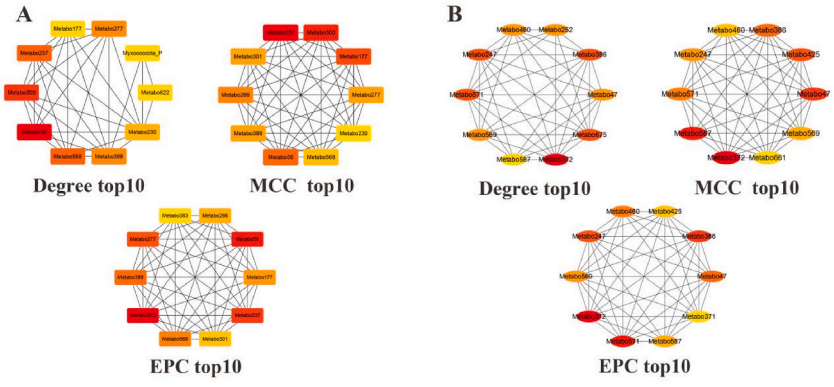


**Fig. 10.** Top 10 of Degree, MCC and EPC in red (A) and green (B) module.

in the treatment of HLYH. The multidisciplinary integration technique for determining the optimal ratio and mechanism of the AB-PL medication pair was successfully established, providing a pharmacological foundation for the clinical prevention of hypertension through the utilization of Chinese medicine.

According to TCM, hypertension with liver yang hyperactivity was the main etiology of hypertension [23]. Symptoms that were present during the initial phase of the illness included dizziness, headaches, ringing in the ears, a bitter taste in the mouth, dryness of the mouth, discomfort and pain in the upper abdomen, restlessness and irritability, flushing, bloodshot eyes, a tongue that appear red, a yellow coating on the tongue, and a pulse that felt stringy [24]. The reduction in NO synthesis led to an increase in peripheral vascular resistance and sustained elevation of blood pressure, resulting in hypertension [25]. Administering L-NAME, a selective inhibitor of NOS, and Aconitum chronically offered a dependable model of HLYH. In our experiment, 6-week L-NAME and Aconitum treatment markedly decreased NO content of the myocardium and significantly induced hypertension and cardiac remodeling with the symptoms of liver-yang hyperactivity obviously.

The well-known complicated makeup and multi-target effects of traditional Chinese herbal medicine bring new opportunities for the potent anti-hypertensive medications [1,26]. Exploring effective management of hypertension from various combinations of these herbs was the encouraging anti-hypertensive research strategy [27,28]. The protective effect of AB and PL on myocardial were well known [7,29]. To our delight, they have produced even more amazing effects when utilized in various combinations. Additionally, the mice of AB-PL (2:3) treatment showed the least irritability. Interestingly, we also discovered that the AB-PL (2:3) treatment significantly reduced MDA content, cardiac remodeling, and blood pressure.

To explore the optimal ratio of AB-PL drug pair for the treatment of HLYH, we further standardized the above experimental data of mice and performed PCA. There were significant variations observed in the levels of the indicators across various groups. Specifically, based on the quantitative analysis results of FPC, AB-PL (2:3) group demonstrated the best preventive effect for HLYH (Fig. 5).

Subsequently, we explored the possible mechanism underlying AB-PL ameliorate hypertension. An 11-module division of metabolites and microbes was established through the creation of a weighted correlation network, by utilizing results from metabolomics and microbiology (Fig. 7). Additionally, the protective effect of AB-PL was closely linked to the metabolites and microbes found in the red and green modules. The pathway analysis for the above metabolites showed that amino acid metabolism (such as arginine metabolism pathway) and lipid metabolism (such as arachidonic acid metabolism) played an important role on the protective mechanism of AB-PL.

Changes in the arginine metabolism pathway were detected in both the red and green modules. Arginine had a complex effect on hypertension. The metabolism of arginine led to the production of different substances, such as NO, urea, creatine, proline, and glutamate, each of which had a distinct impact on the development of hypertension. Maintaining vascular homeostasis relied heavily on the arginine-NO pathway. The guanylate cyclase pathway allowed for the diffusion of NO into vascular smooth muscle cells, resulting in vasodilation [30]. Studies have shown that inhibiting NO synthesis worsens hypertension [31]. Conversely, if the bioavailability of NO increased, it could result in antihypertensive effects and weakening damage to target organs [32]. Additionally, abnormalities in arginine and proline metabolism pathways were observed. Glutamate could undergo interconversion with proline, which was a specific secondary amino acid. Glutamate had the ability to produce glutamate-semialdehyde and could be transformed into ornithine, which served as a precursor for the synthesis of arginine in the urea cycle [33]. Alternatively, pyrroline-5-carboxylate was generated from glutamate-semialdehyde and subsequently transformed into proline. Studies have demonstrated that arginase had the ability to convert arginine into ornithine along with urea. Enhanced expression of arginase led to a decrease in the synthesis of NO while facilitating the production of glutamate and proline [34,35]. The detection of disrupted arginine biosynthesis and arginine/-proline metabolism in the metabolomic analysis of mouse feces suggested that it might have negatively affected endothelial function by diminishing the bioactivity of NO. This pathway could have been crucial in regulating hypertension. Furthermore, studies had also shown a close relationship between histidine and phenylalanine metabolism and hypertensive myocardial hypertrophy. Oral histidine supplementation could alter thiamine metabolism, and arginine biosynthesis, and produce effects on taurine and hypotaurine metabolism. The addition of taurine could enhance the bioavailability of NO, consequently leading to a decrease in hypertension [36]. The administration of phenylalanine effectively reduced the increase in blood pressure associated with aging in rats with spontaneous hypertension [37]. Bile acids could induce hypertension by increasing the production of aldosterone and corticosterone in blood vessels, enhancing vasoconstrictor responses [38].

In addition, disruptions in fatty acid metabolism were also closely associated with hypertension. Analysis of mouse fecal metabolomics revealed alterations in the metabolism of arachidonic acid and glycerophospholipids. It was reported that endothelial cells had the ability to impede the process of fatty acid oxidation, consequently impacting signal transduction [39,40]. Therefore, AB-PL showed a protective effect on L-NAME-induced hypertension, which could be attributed to the alterations in fatty acid metabolism, as it prevented the impairment of endothelial cell function.

To further explore the protective mechanism of AB-PL, network topology analysis was adopted to reveal its key nodes. 135 metabolites and 23 microbiotas were recommend as potentially important targets for the protective effect of AB-PL in HLYH. On the one hand, many investigations suggest that the presence of Clostridium and RF39 in the red module and Ligilactobacillus in the green module can inhibit the increase in blood pressure and affect the development of hypertension. Therefore, its effect on HLYH may be an important mechanism for AB-PL [41–43]. On the other hand, key metabolites such as β-alanyl-L-lysine, valine, and glycylleucine, as well as tetradecanoylcarnitine, stearoylcarnitine, and levocarnitine in the green module, were likely involved in amino acid metabolism, fatty acid metabolism, and energy metabolism. These metabolites may be associated with anti-inflammatory and antioxidant properties [44]. However, research on this aspect was still relatively limited, and more studies were needed to confirm their specific mechanisms of action and effects.

## 5. Conclusion

In summary, the findings revealed the synergistic effect of AB-PL for preventing HLYH and the 2:3 ratio of AB-PL was ideal. In addition, the key factors for AB-PL preventing hypertension might have been associated with 135 metabolites (involving amino acid metabolism and lipid metabolism) and 23 microorganisms (such as clostridium and etc.) (Fig. 11). This study established an effective foundation of herbal remedies compatibility for hypertension and enhancing the integration of TCM approaches and providing reference on clinical application of AB-PL compatibility.

## Data availability

The data used to support the findings of this study are available from the corresponding author upon request.

## Funding statement

This work was supported by National Natural Science Foundation of China (82074148, 82104173), Science and Technology Department of Heilongjiang Province (LH2022H110, LH2022H112) and Postdoctoral Scientific Research Foundation of Hei longjiang Province (LBH-Q18128) National Innovation and Entrepreneurship Training Program for College Students (202211230036) and

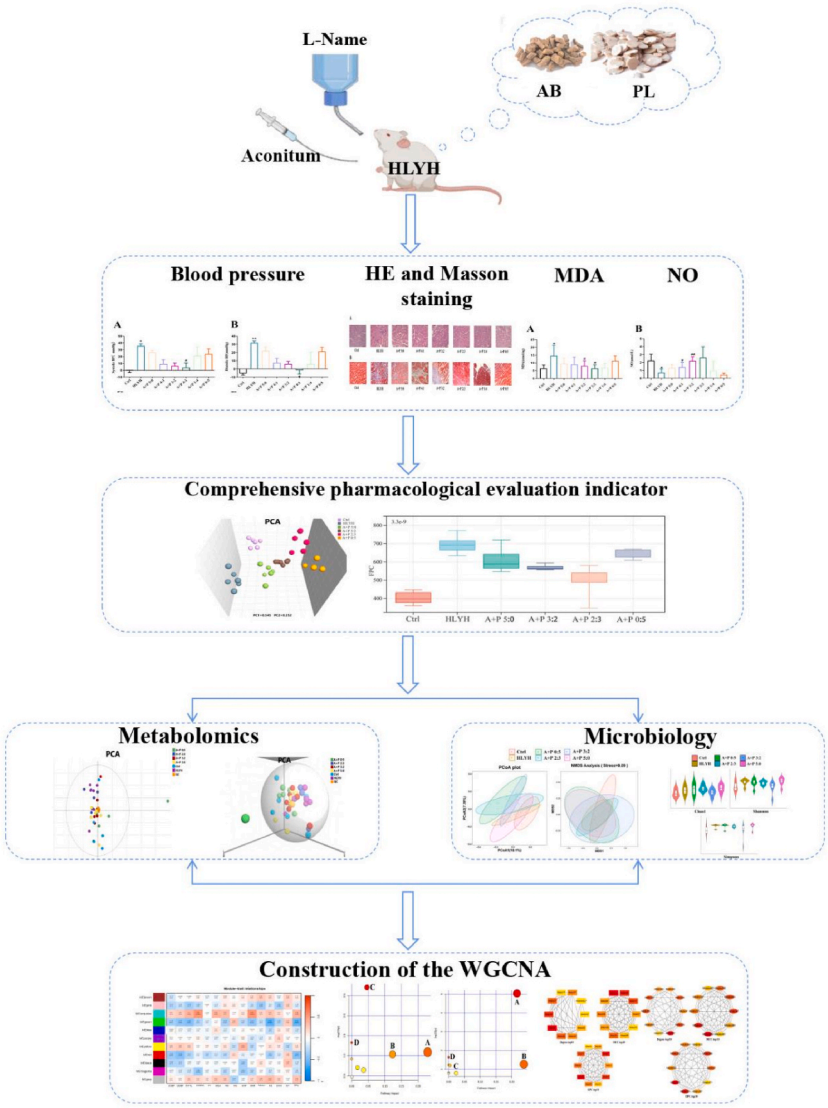


**Fig. 11.** The AB-PL (2:3) plays the ideal synergistic effect on preventing HLYH, the key factors for AB-PL preventing hypertension might been associated with 135 metabolites (involving amino acid metabolism and lipid metabolism) and 23 microorganisms.

Innovation and Entrepreneurship Training Program for College Students of Heilongjiang Province (S202211230045) and Graduate Innovation Fund Projects of Qiqihar Medical University (QYYCX2022-19, QYYCX2022-21).

## CRediT authorship contribution statement

**Yanyan Zhang:** Writing – original draft, Methodology, Investigation, Conceptualization. **Peimei Yan:** Methodology, Investigation, Conceptualization. **Yuhui He:** Methodology, Conceptualization. **Shan Ren:** Methodology, Investigation. **Dingxiao Wu:** Investigation. **Yingwanqi Wang:** Investigation. **Siyao Song:** Investigation. **Peng Lu:** Investigation. **Xue Li:** Investigation. **Guangwei Li:** Methodology. **Weiwei Jia:** Methodology. **Ying Lyu:** Methodology. **Haiying Dong:** Formal analysis, Data curation. **Dan Xiao:** Software, Formal analysis. **Lin Ding:** Methodology, Investigation. **Song Lin:** Writing – review & editing, Conceptualization. **Yan Lin:** Writing – review & editing, Conceptualization.

## Declaration of competing interest

The authors declare that they have no known competing financial interests or personal relationships that could have appeared to influence the work reported in this paper.

## Glossary

| | |
|---|---|
| AB | *Achyranthes bidentata* Blume |
| PL | Paeonia lactiflora Pall. |
| Aconitum | Aconitum carmichaelii Debeaux |
| PCA | principal component analysis |
| WGCNA | weighted correlation network analysis |
| TCM | Traditional Chinese Medicine |
| ZGFD | Zhen Gan Xi Feng decoction |
| HLYH | hypertension with liver yang hyperactivity syndrome |
| MDA | malondialdehyde |
| FPC | first principal component |
| SEM | standard error of mean |
| MM | module membership |
| SBP | systolic blood pressure differential |
| DBP | diastolic blood pressure differential |
| HW/TL | heart weight/tibia length |
| HW/BW | heart weight/body weight ratio |
| FT | face temperature |
| HR | heart rate |
| NO | nitric oxide |
| ANP | atrial natriuretic peptide |
| BNP | brain natriuretic peptide |
| Masson | masson staining |
| HE | hematoxylin-eosin staining |
| CVF | collagen volume fraction |
| DWV | drinking water volume |
| RT | rotation time |

## Appendix A. Supplementary data

Supplementary data to this article can be found online at https://doi.org/10.1016/j.heliyon.2024.e38649.

## References

[1] S.C. Da, I. Guedes, J. de Lima, J. Sobrinho, S.A. Dos, Responses triggered by the immune system in hypertensive conditions and repercussions on target organ damage: a review, Curr. Cardiol. Rev. 19 (2023) e200922208959, https://doi.org/10.2174/1573403X18666220920090632.
[2] Y. Zhang, B. Wang, C. Ju, et al., Traditional Chinese medicine for essential hypertension: a clinical evidence map, Evid Based Complement Alternat Med 2020 (2020) 5471931, https://doi.org/10.1155/2020/5471931.
[3] Y. Huang, Y. Chen, H. Cai, et al., Herbal medicine (zhengan xifeng decoction) for essential hypertension protocol for a systematic review and meta-analysis, Medicine (Baltim.) 98 (2019) e14292, https://doi.org/10.1097/MD.0000000000014292.
[4] X.P. Lai, Research on the Clinical Efficacy and Life Quality of Zhengan Xifeng Decoction on Liver-And-Kidney Yin Deficiency Hypertension, 2021.

[5] X. Huang, S. Ngaenklangdon, J. He, X. Gao, Traditional Chinese medicine's liver yang ascendant hyperactivity pattern of essential hypertension and its treatment approaches: a narrative review, Compl. Ther. Clin. Pract. 43 (2021) 101354, https://doi.org/10.1016/j.ctcp.2021.101354.

[6] X. Wu, X. Jiang, Systematic review and meta analysis of randomized controlled trials on tianmagouteng decoction in treatment of primary hypertension with liver yang hyperactivity syndrome, J. Tradit. Chin. Med. 33 (2013) 15–18, https://doi.org/10.1016/s0254-6272(13)60094-1.

[7] L.H. Deng, W. Liu, Y.Q. Zhao, Clinical application of bloodletting effect of achyrantheson hypertension, Liaoning Journal of Traditional Chinese Medicine 47 (2020) 195–197, https://doi.org/10.13192/j.issn.1000-1719.2020.01.059.

[8] Q.Q. Dai, H. Xia, G.Y. Xia, et al., Research progress on mechanism of radix paeoniae alba decotion and total glucosides of paeiny, Modernization of Traditional Chinese Medicine and Materia Medica-World Science and Technology 22 (2020) 39–46, https://doi.org/10.11842/wst.20200210002.

[9] J.Y. Yang, G.J. Liu, B.Y. Liu, et al., A series of lectures on authentic Chinese medicinal materials (2) the research status of authentic Chinese medicinal materials paeonia lactiflora, Modern Medicine and Health Research Electronic Journal 4 (2020) 160–162.

[10] S.J. Yang, A.J. Feng, Y. Sun, L. Zhang, F.M. Bo, L.J. Li, Research progress on mechanism and pharmacological activities of total glucosides of paeony, Chinese Journal of Modern Applied Pharmacy 38 (2021) 1627–1633, https://doi.org/10.13748/j.cnki.issn1007-7693.2021.13.015.

[11] Y.L. Zhang, Y. Tian, Q.F. Fu, et al., Research progress of chemical constituents and pharmacological action of paeonia tactilora pall, Acta Chinese Medicine and Pharmacology 49 (2021) 104–109, https://doi.org/10.19664/j.cnki.1002-2392.210047.

[12] H. Dong, S. Zhang, W. Du, H. Cong, L. Zhang, Pharmacodynamics and metabonomics study of tianma gouteng decoction for treatment of spontaneously hypertensive rats with liver-yang hyperactivity syndrome, J. Ethnopharmacol. 253 (2020) 112661, https://doi.org/10.1016/j.jep.2020.112661.

[13] S.M. Greish, Z. Abdel-Hady, S.S. Mohammed, et al., Protective potential of curcumin in l-name-induced hypertensive rat model: at1r, mitochondrial dna synergy, Int J Physiol Pathophysiol Pharmacol 12 (2020) 134–146.

[14] X.J. Zhang, T.C. Sun, Z.W. Liu, F.J. Wang, Y.D. Wang, J. Liu, Effects of tianmagouteng particles on brain cognitive function in spontaneously hypertensive rats with hyperactivity of liver-yang: a [f-18] fdg micro-pet imaging study, Biomed. Pharmacother. 95 (2017) 1838–1843, https://doi.org/10.1016/j.biopha.2017.08.100.

[15] S. Chen, Y. Lv, H. Wu, N. Chen, X. Chen, X. Tang, Effect of qianyang recipe on correlated indices of hypertension rats of gan-yang hyperactivity syndrome, Chin. J. Integr. Tradit. West. Med. 31 (2011) 973–976.

[16] Z. Li, M. Wu, D. Liu, et al., Pingyang jiangya fang pretreatment reduces the blood pressure of spontaneously hypertensive rats with liver-yang hyperactivity syndrome via ros/akt oxidative stress pathway, Ann. Palliat. Med. 10 (2021) 1904–1919, https://doi.org/10.21037/apm-20-1371.

[17] G.Y. Shang, L. Zhang, L. Lin, et al., Toward the development of personalized syndrome discriminant systems: a discriminant system for hypertension with liver yang hyperactivity syndrome, Evid Based Complement Alternat Med 2021 (2021) 4532279, https://doi.org/10.1155/2021/4532279.

[18] L.H. Yang, S.Z. Zou, Y.X. Li, A new instrument and method for noninvasive measurement of systolic and diastolic blood pressure in rats, Chin. J. Appl. Physiol. (1991) 64–66, https://doi.org/10.13459/j.cnki.cjap.1991.01.015.

[19] P. Langfelder, S. Horvath, Wgcna: an r package for weighted correlation network analysis, BMC Bioinf. 9 (2008) 559, https://doi.org/10.1186/1471-2105-9-559.

[20] G.D. Bader, C.W. Hogue, An automated method for finding molecular complexes in large protein interaction networks, BMC Bioinf. 4 (2003) 2, https://doi.org/10.1186/1471-2105-4-2.

[21] C.H. Chin, S.H. Chen, H.H. Wu, C.W. Ho, M.T. Ko, C.Y. Lin, Cytohubba: identifying hub objects and sub-networks from complex interactome, BMC Syst. Biol. 8 (Suppl 4) (2014) S11, https://doi.org/10.1186/1752-0509-8-S4-S11.

[22] J. Kwiecinski, R.J. Lennen, G.A. Gray, et al., Progression and regression of left ventricular hypertrophy and myocardial fibrosis in a mouse model of hypertension and concomitant cardiomyopathy, J. Cardiovasc. Magn. Reson. 22 (2020) 57, https://doi.org/10.1186/s12968-020-00655-7.

[23] X.T. Xu, Y. Tang, Study on the distribution regularity of tcm syndrome types of hypertension, Clinical Journal of Chinese Medicine 14 (2022) 86–89.

[24] G.Y. Shang, L. Zhang, L. Lin, et al., Toward the development of personalized syndrome discriminant systems: a discriminant system for hypertension with liver yang hyperactivity syndrome, Evid Based Complement Alternat Med 2021 (2021) 4532279, https://doi.org/10.1155/2021/4532279.

[25] I.R. Barrows, A. Ramezani, D.S. Raj, Inflammation, immunity, and oxidative stress in hypertension-partners in crime? Adv. Chron. Kidney Dis. 26 (2019) 122–130, https://doi.org/10.1053/j.ackd.2019.03.001.

[26] P. Maneesai, N. Chaihongsa, M. Iampanichakul, et al., Clitoria ternatea (linn.) Flower extract attenuates vascular dysfunction and cardiac hypertrophy via modulation of ang ii/at(1) r/tgf-beta1 cascade in hypertensive rats, J. Sci. Food Agric. 102 (2022) 2253–2261, https://doi.org/10.1002/jsfa.11563.

[27] G. Hou, Y. Jiang, Y. Zheng, et al., Mechanism of radix astragali and radix salviae miltiorrhizae ameliorates hypertensive renal damage, BioMed Res. Int. 2021 (2021) 5598351, https://doi.org/10.1155/2021/5598351.

[28] Q. Zhang, J. Yang, C. Yang, X. Yang, Y. Chen, Eucommia ulmoides oliver-tribulus terrestris l. Drug pair regulates ferroptosis by mediating the neurovascular-related ligand-receptor interaction pathway- a potential drug pair for treatment hypertension and prevention ischemic stroke, Front. Neurol. 13 (2022) 833922, https://doi.org/10.3389/fneur.2022.833922.

[29] C. Yang, J. Cheng, Q. Zhu, Q. Pan, K. Ji, J. Li, Review of the protective mechanism of paeonol on cardiovascular disease, Drug Des. Dev. Ther. 17 (2023) 2193–2208, https://doi.org/10.2147/DDDT.S414752.

[30] M. Li, Y. Wu, L. Ye, The role of amino acids in endothelial biology and function, Cells 11 (2022), https://doi.org/10.3390/cells11081372.

[31] N.S. Bryan, Nitric oxide deficiency is a primary driver of hypertension, Biochem. Pharmacol. 206 (2022) 115325, https://doi.org/10.1016/j.bcp.2022.115325.

[32] A.W. Abukhodair, W. Abukhudair, M.S. Alqarni, The effects of l-arginine in hypertensive patients: a literature review, Cureus 13 (2021) e20485, https://doi.org/10.7759/cureus.20485.

[33] Y. Shen, Y. Zhang, W. Li, K. Chen, M. Xiang, H. Ma, Glutamine metabolism: from proliferating cells to cardiomyocytes, Metabolism 121 (2021) 154778, https://doi.org/10.1016/j.metabol.2021.154778.

[34] H. Li, C.J. Meininger, J.J. Hawker, et al., Regulatory role of arginase i and ii in nitric oxide, polyamine, and proline syntheses in endothelial cells, Am. J. Physiol. Endocrinol. Metab. 280 (2001) E75–E82, https://doi.org/10.1152/ajpendo.2001.280.1.E75.

[35] J. Pernow, C. Jung, Arginase as a potential target in the treatment of cardiovascular disease: reversal of arginine steal? Cardiovasc. Res. 98 (2013) 334–343, https://doi.org/10.1093/cvr/cvt036.

[36] Q. Sun, B. Wang, Y. Li, et al., Taurine supplementation lowers blood pressure and improves vascular function in prehypertension: randomized, double-blind, placebo-controlled study, Hypertension 67 (2016) 541–549, https://doi.org/10.1161/HYPERTENSIONAHA.115.06624.

[37] Z. Wang, C. Cheng, X. Yang, C. Zhang, L-phenylalanine attenuates high salt-induced hypertension in dahl ss rats through activation of gch1-bh4, PLoS One 16 (2021) e0250126, https://doi.org/10.1371/journal.pone.0250126.

[38] Y. Zhu, X. Shui, Z. Liang, et al., Gut microbiota metabolites as integral mediators in cardiovascular diseases, Int. J. Mol. Med. 46 (2020) 936–948, https://doi.org/10.3892/ijmm.2020.4674, submitted for publication.

[39] F. Patella, Z.T. Schug, E. Persi, et al., Proteomics-based metabolic modeling reveals that fatty acid oxidation (fao) controls endothelial cell (ec) permeability, Mol. Cell. Proteomics 14 (2015) 621–634, https://doi.org/10.1074/mcp.M114.045575.

[40] J. Kalucka, L. Bierhansl, N.V. Conchinha, et al., Quiescent endothelial cells upregulate fatty acid beta-oxidation for vasculoprotection via redox homeostasis, Cell Metabol. 28 (2018) 881–894.e13, https://doi.org/10.1016/j.cmet.2018.07.016.

[41] X. Luo, Z. Han, Q. Kong, Y. Wang, H. Mou, X. Duan, Clostridium butyricum prevents dysbiosis and the rise in blood pressure in spontaneously hypertensive rats, Int. J. Mol. Sci. 24 (2023), https://doi.org/10.3390/ijms24054955.

[42] H. Bai, R.J. Gu, L.Y. Chen, et al., Electroacupuncture interventions alleviates myocardial ischemia reperfusion injury through regulating gut microbiota in rats, Microvasc. Res. 138 (2021) 104235, https://doi.org/10.1016/j.mvr.2021.104235.
[43] M. Mukohda, T. Yano, T. Matsui, et al., Treatment with ligilactobacillus murinus lowers blood pressure and intestinal permeability in spontaneously hypertensive rats, Sci. Rep. 13 (2023) 15197, https://doi.org/10.1038/s41598-023-42377-7.
[44] D.M. Zhang, Z.X. Guo, Y.L. Zhao, et al., L-carnitine regulated nrf2/keap1 activation in vitro and in vivo and protected oxidized fish oil-induced inflammation response by inhibiting the nf-kappab signaling pathway in rhynchocypris lagowski dybowski, Fish Shellfish Immunol. 93 (2019) 1100–1110, https://doi.org/10.1016/j.fsi.2019.08.041.